ELSEVIER

Biophysical Chemistry 70 (1998) 133–146

Biophysical Chemistry

An improved approximate solution of the Lamm equation for the simultaneous estimation of sedimentation and diffusion coefficients from sedimentation velocity experiments

Joachim Behlke *, Otto Ristau

Max Delbrueck Center for Molecular Medicine, Berlin 13122, Germany

Received 23 June 1997; revised 16 October 1997; accepted 16 October 1997

Abstract

Sedimentation and diffusion coefficients are important parameters to describe size and shape of macromolecules in solution. The data can be obtained from sedimentation velocity experiments by a nonlinear fitting procedure using approximate solutions for the Lamm equation. Here, we present a modification of such a model function that was originally proposed by Fujita [H. Fujita, Mathematical Theory of Sedimentation Analysis, Wiley, New York, 1962]. The extended model function is well suitable to study low molecular mass compounds. The improvement of this solution given here is based on using an adjustable value for the explicit integration variable, z, the reduced radius. This modification leads to more accurate sedimentation and diffusion coefficients compared to using a constant value of 0.5 as used by Fujita. The advantage of our modification was demonstrated by the analysis of noise-free curves calculated using the finite element method, as well as experimental curves obtained for the peptides angiotensin I and II. The relatively low sedimentation and diffusion coefficients found for both substances indicate that the peptides exist as extended chains of about 3.65 nm (angiotensin I) or 3.04 nm length (angiotensin II) in solution. The lack of higher-order structure of the peptides that was derived also from CD spectra might facilitate receptor binding, and could be one reason for the fast proteolytic digestion of the free peptides. © 1998 Elsevier Science B.V.

Keywords: Sedimentation; Diffusion; Lamm equation; Gross conformation; Nonlinear fit; Angiotensin

1. Introduction

Hydrodynamic methods are important for characterizing the structure of biological macromolecules or their complexes in solution [1,2]. Together with the sedimentation coefficients, the corresponding data for the diffusion allow us to estimate the size and shape of the substances. Moreover, the diffusion coefficients are of practical interest to analyze fast reactions, e.g., between proteins and smaller molecules or ligands with rate constants $> 10^6$ M^{-1} s^{-1} [3]. Many protein ligand reactions proceed with diffusion-controlled kinetics [4,5]. In such interaction

* Corresponding author. Max Delbrueck Center for Molecular Medicine, Robert Roessle Str. 10, 13122 Berlin, Germany. Tel.: + 49-30-9406-2205; fax: + 49-30-9406-2802; e-mail: behlke@mdc-berlin.de

PII S0301-4622(97)00124-5

processes, the association rate is limited by the time it takes to bring the reactants together by diffusion [6]. Recently, new techniques were developed to estimate diffusion coefficients (see also Ref. [5]). In contrast, the classical method of analytical ultracentrifugation allows us to determine simultaneously sedimentation coefficients and therefore the molecular mass of the substances of interest.

Closed analytical solutions for the transport equation (Lamm equation [7]) for the ultracentrifuge are not available. However, in the sixties, Fujita [8] has derived some approximate solutions for the Lamm equation. One of these functions (Eq. 2.280 in Ref. [8]) is particularly well suited for the direct determination of sedimentation and diffusion coefficients of small proteins with a molecular mass of 10–20 kDa [9] or lower. The data can be obtained directly by a nonlinear fit of the radial concentration distributions using the above-mentioned equation. The particular advantage of the Archibald type solution of the Lamm equation is based on the fact that it does not require a plateau region as is necessary for the Faxén type solutions. Although the model function (Eq. 2.280 in Ref. [8]) accounts for both boundaries at the meniscus, as well as the cell base, the equation does not allow an optimal fit of the curves near the meniscus [9]. The aim of the present study was the improvement of the Fujita equation to obtain a model function allowing the optimal determination of sedimentation and diffusion coefficients of macromolecules. Moreover, it was also desirable to analyze low molecular mass solutes of a few hundred Daltons such as the peptides angiotensin I (Ang I) and angiotensin II (Ang II). For solving this problem, a derivation of the model function was necessary to analyze the influence of several parts of the equation on the accuracy to fit the curves.

2. Theory

The Lamm equation (Eq. (1)) described the radial (r) concentration (c) distribution for sector-shaped cells in a sedimentation velocity experiment,

$$\frac{\partial C}{\partial t} = \frac{1}{r}\frac{\partial}{\partial r}\left[rD\frac{\partial C}{\partial r} - s\omega^2 rC \right] \tag{1}$$

with s the sedimentation coefficient, D the diffusion coefficient and ω the angular velocity. The initial and boundary conditions are given by Eq. (2). The initial condition describes the uniform concentration C_0 at the beginning of the experiment, whereas the boundary conditions take into account that no solute can pass through the air–liquid meniscus or the cell bottom.

$$\begin{array}{llll} C = C_0; & t = 0 & r_0 < r < r_b & \text{initial condition} \\ D\dfrac{\partial C}{\partial r} = r\omega^2 sC; & t > 0 & r = r_0 & \text{meniscus boundary condition} \\ D\dfrac{\partial C}{\partial r} = r\omega^2 sC; & t > 0 & r = r_b & \text{bottom boundary condition} \end{array} \tag{2}$$

r_0 stands for the meniscus and r_b the bottom position. With the following substitutions

$$\theta = \frac{C}{C_0};\ x = \left(\frac{r}{r_0}\right)^2;\ \tau = 2s\omega^2 t;\ \varepsilon = \frac{2D}{s\omega^2 r_0^2} \tag{3}$$

we obtain a dimensionless Lamm equation

$$\frac{\partial\theta}{\partial\tau} = \frac{\partial}{\partial x}\left[x\left(\varepsilon\frac{\partial\theta}{\partial x} - \theta \right)\right] \tag{4}$$

This variant of Lamm equation is suitable for a Faxén type solution obtained by Holladay [10]. The initial and boundary conditions are transformed to:

$$\begin{array}{llll} \theta = 1; & \tau = 0 & 1 < x < \infty & \text{initial condition} \\ \varepsilon\dfrac{\partial\theta}{\partial x} = \theta; & \tau > 0 & x = 1 & \text{meniscus boundary condition} \end{array} \tag{5}$$

Moreover, when substituting θ by $e^{-\tau^*}U$, the following expression is obtained.

$$\frac{\partial U}{\partial\tau} = \varepsilon x\frac{\partial^2 U}{\partial x^2} + (\varepsilon - x)\frac{\partial U}{\partial x} \tag{6}$$

To obtain an approximate solution of the Lamm equation of the Archibald type that accounts for both boundaries at the meniscus and at the cell bottom, we have to transform the variable x:

$$\begin{array}{llll} x = z(x_b - 1) + 1 & \text{respectively} & z = \dfrac{x-1}{x_b - 1} & \\ & & 0 < z < 1 & \\ \partial x = (x_b - 1)\partial z; & & x_b = \left(\dfrac{r_b}{r_0}\right)^2 & \end{array} \tag{7}$$

With this substitution, Eq. (6) becomes:

$$\frac{\partial U}{\partial t} = \frac{\varepsilon}{(x_b - 1)}\left[\frac{z(x_b - 1) + 1}{x_b - 1}\right]\frac{\partial^2 U}{\partial z^2} + \left[\frac{\varepsilon}{(x_b - 1)} - \frac{z(x_b - 1) + 1}{x_b - 1}\right]\frac{\partial U}{\partial z} \quad (8)$$

To get an analytical solution, the explicit variable z will be held constant on an arbitrary value within the integration region. For a further calculation, we have to make the substitutions:

$$e = \frac{\varepsilon}{x_b - 1} \text{ and } a = \frac{z(x_b - 1) + 1}{(x_b - 1)} \quad (9)$$

The value of z and therefore of a will be considered later. Eq. (8) can be simplified as follows:

$$\frac{\partial U}{\partial \tau} = ae\frac{\partial^2 U}{\partial z^2} + (e - a)\frac{\partial U}{\partial z} \quad (10)$$

Furthermore, when substituting

$$U = \upsilon \exp\left(-\frac{2z(e - a) + \tau(e - a)^2}{4ac}\right) \quad (11)$$

one obtains the normal form of the differential equation

$$\frac{\partial \upsilon}{\partial \tau} = ae\frac{\partial^2 \upsilon}{\partial z^2} \quad (12)$$

Now the initial conditions are transformed to:

$$\upsilon = \exp\left(-\frac{z(a - e)}{2ae}\right);\ \tau = 0;\ 0 < z < 1 \quad (13)$$

and the new boundary conditions read:

$$\frac{\partial \upsilon}{\partial z} = \upsilon\left(\frac{a + e}{2ae}\right);\ \tau > 0 \text{ for } z = 0 \text{ and } z = 1 \quad (14)$$

The Laplace transformation according to τ considering p as the Laplace variable gives the subsidiary Eq. (15):

$$\frac{\partial^2 \bar{\upsilon}}{\partial z^2} - q^2\bar{\upsilon} = -\frac{1}{ae}\exp\left(-z\frac{(a - e)}{2ae}\right) \quad \text{with } q^2 = \frac{p}{ae} \quad (15)$$

The general solution of the differential equation reads:

$$\bar{\upsilon} = \frac{1/(ae)}{q^2 - [(a - e)/2ae]^2}\exp\left(-\frac{z(a - e)}{2ae}\right) + c_1\exp(-qz) + c_2\exp(qz) \quad (16)$$

Here, c_1 and c_2 are the integration constants.

This equation can be simplified by the substitutions:

$$b = \frac{1}{2ae};\ \alpha = a - e \text{ and } \gamma = a + e \quad (17)$$

to obtain the general solution of Eq. (15) in the following form:

$$\bar{\upsilon} = \frac{2b}{q^2 - (\alpha b)^2}\exp(-z\alpha b) + c_1\exp(-qz) + c_2\exp(qz) \quad (18)$$

To introduce the boundary conditions we have to differentiate this equation according to z:

$$\frac{\partial \bar{\upsilon}}{\partial z} = -\frac{2\alpha b^2}{q^2 - (\alpha b)^2}\exp(-z\alpha b) - c_1 q\exp(-qz) - c_1 + c_2 q\exp(qz) \quad (19)$$

When considering only one boundary condition, e.g., near the meniscus where $z = 0$, Eq. (19) becomes a Faxén type solution with $c_2 = 0$:

$$\frac{\partial \bar{\upsilon}}{\partial z} = -\frac{2\alpha b^2}{q^2 - (\alpha b)^2} - c_1 q \quad (20)$$

Now the meniscus boundary condition (14) allows the determination of c_1:

$$c_1 = -\frac{2b^2(\alpha + \gamma)}{\left(q^2 - (\alpha b)^2\right)(q + \gamma b)} \quad (21)$$

When considering only the front boundary and the

initial condition, the solution for the differential Eq. (15) reads:

$$\bar{v} = \frac{2b}{q^2 - (\alpha b)^2}\exp(-z\alpha b) - \frac{2b^2(\alpha+\gamma)\exp(-qz)}{\left(q^2-(\alpha b)^2\right)(q+\gamma b)} \quad (22)$$

After splitting up in partial fractions the solution becomes:

$$v = \frac{2b}{q^2 - (\alpha b)^2}\exp(-z\alpha b) + \frac{(\alpha+\gamma)\exp(-qz)}{\alpha(\gamma-\alpha)(q+\alpha b)} - \frac{\exp(-qz)}{\alpha(q-\alpha b)} - \frac{2\exp(-qz)}{(\gamma-\alpha)(q+\gamma b)} \quad (23)$$

The inverse transform of $\bar{v}$ [11] leads to Eq. (24):

$$v = \exp\left(\frac{a^2\tau - 2z\alpha}{4ae}\right) - \frac{\alpha}{2e}\exp\left(\frac{\alpha^2\tau + 2\alpha z}{4ae}\right)\operatorname{erfc}\left(\frac{z+\alpha\tau}{2\sqrt{ae\tau}}\right) - \frac{1}{2}\exp\left(\frac{\alpha^2\tau - 2z\alpha}{4ae}\right)\operatorname{erfc}\left(\frac{z-\alpha\tau}{2\sqrt{ae\tau}}\right) + \frac{\gamma}{2e}\exp\left(\frac{\gamma^2\tau + 2z\gamma}{4ae}\right)\operatorname{erfc}\left(\frac{z+\gamma\tau}{2\sqrt{ae\tau}}\right) \quad (24)$$

Here, erfc means the complementary error function.

$$\operatorname{erfc}(z) = 1 - \operatorname{erf}(z)$$

For the concentration C we obtain:

$$C = \frac{C_0}{2}e^{-\tau}\left\{2 - \frac{\alpha}{e}\exp\left(\frac{z\alpha}{ae}\right)\operatorname{erfc}\left(\frac{z+\alpha\tau}{2\sqrt{ae\tau}}\right) - \operatorname{erfc}\left(\frac{z-\alpha\tau}{2\sqrt{ae\tau}}\right) + \frac{\gamma}{e}\exp\left(\frac{(\gamma^2-\alpha^2)+2z(\alpha+\gamma)}{4ae}\right) \times \operatorname{erfc}\left(\frac{z+\gamma\tau}{2\sqrt{ae\tau}}\right)\right\} \quad (25)$$

When considering only the bottom boundary condition ($c_1 = 0$) Eq. (16) is transformed to:

$$\bar{v} = \frac{2b}{q^2 - (\alpha b)^2}\exp(-z\alpha b) + c_2\exp(q)\exp(-q(1-z)) \quad (26)$$

By means of the bottom boundary condition (14) for c_2, we obtain the following expression:

$$c_2 = \frac{2b^2(\alpha+\gamma)\exp(-\alpha b)\exp(-q)}{\left(q^2-(\alpha b)^2\right)(q-\gamma b)} \quad (27)$$

The solution for the differential Eq. (15) considering only the boundary condition at the cell bottom reads:

$$\bar{v} = \frac{2b\,\exp(-z\alpha b)}{\left(q^2-(\alpha b)^2\right)} + \frac{2b^2(\alpha+\gamma)\exp(-\alpha b)\exp(-q(1-z))}{\left(q^2-(\alpha b)^2\right)(q-\gamma b)} \quad (28)$$

After splitting up in partial fractions we obtain:

$$\bar{v} = \frac{2b\,\exp(-z\alpha b)}{\left(q^2-(\alpha b)^2\right)} + \frac{\exp(-\alpha b)\exp(-q(1-z))}{\alpha(q+\alpha b)} - \frac{(\alpha+\gamma)\exp(-\alpha b)\exp(-q(1-z))}{\alpha(\gamma-\alpha)(q-\alpha b)} + \frac{2\exp(-\alpha b)\exp(-q(1-z))}{(\gamma-\alpha)(q-\gamma b)} \quad (29)$$

For the function v, we obtain the following expression:

$$v = \exp\left(\frac{\alpha^2\tau - 2z\alpha}{4ae}\right) - \frac{1}{2}\exp\left(\frac{\alpha^2\tau + 2\alpha(1-z) - 2\alpha}{4ae}\right) \times \operatorname{erfc}\left(\frac{(1-z)+\alpha\tau}{2\sqrt{ae\tau}}\right) - \frac{a}{2e}\exp\left(\frac{\alpha^2\tau - 2\alpha(1-z) - 2\alpha}{4ae}\right) \times \operatorname{erfc}\left(\frac{(1-z)-\alpha\tau}{2\sqrt{ae\tau}}\right) - \frac{\gamma}{2e}\exp\left(\frac{\gamma^2\tau - 2\gamma(1-z) - 2\alpha}{4ae}\right) \times \operatorname{erfc}\left(\frac{(1-z)-\gamma\tau}{2\sqrt{ae\tau}}\right) \quad (30)$$

The function describing the radial concentration distribution is given by:

$$C = \frac{C_0}{2}e^{-\tau}\left\{2 - \operatorname{erfc}\left(\frac{(1-z)+\alpha\tau}{2\sqrt{ae\tau}}\right) - \frac{\alpha}{e}\exp\left(\frac{-\alpha(1-z)}{ae}\right)\operatorname{erfc}\left(\frac{(1-z)-\alpha\tau}{2\sqrt{ae\tau}}\right) + \frac{\gamma}{e}\exp\left(\frac{(\gamma^2-\alpha^2)\tau - 2(\alpha+\gamma)(1-z)}{4ae}\right) \times \operatorname{erfc}\left(\frac{(1-z)-\gamma\tau}{2\sqrt{ae\tau}}\right)\right\} \quad (31)$$

A simultaneous consideration of both boundary conditions using the Laplace method is possible, but in this case the inverse transformation to a closed analytical solution is not possible. However, the examination of the rear solution from the numerical point of view demonstrates that this solution possesses only a very small influence on the front boundary condition. Contrary to this behavior, the solution with the meniscus boundary condition influences scarcely also the bottom boundary condition. This can be explained in the following way: the concentration and the slope dc/dr of the rear solution at the meniscus is nearly zero. On the other hand, the concentration and the slope dc/dr for the front solution yields also very small values at the bottom (see also Fig. 1). Therefore, a suitable solution for a simplified Lamm equation with the simultaneous consideration of both boundary conditions can be found when the front solution as Laplace transform is obtained first. After this step (but not

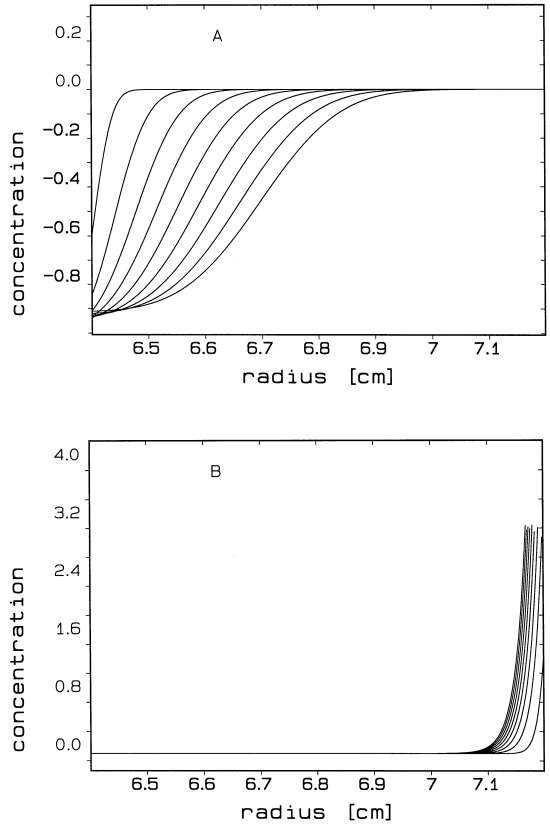

Fig. 1. Scheme of the radial concentration distribution calculated (A) by Eq. (25) considering the front boundary condition only or (B) using Eq. (31), taking into account the rear boundary condition only. The influence of the initial concentration C_0 of the front solution on the rear boundary condition is zero because the initial condition was already included in the rear boundary condition. The same argument is valid for the influence of the initial concentration of the rear solution on the front boundary condition vice versa. Therefore, the initial concentration (value 2 of the first term) but not the initial condition, was deleted in both diagrams. As a consequence, negative concentration values occur, but the concentration and slope in the corresponding boundary regions are zero as supposed.

simultaneously) the rear boundary condition has to be introduced.

As general solution of the Lamm equation (Eq. (12)), we use Eq. (16) and introduce for the first integration constant c_1 Eq. (21). The second integration constant will now be determined by the rear boundary condition.

$$\bar{v} = \frac{2b}{q^2 - (\alpha b)^2}\exp(-z\alpha b) - \frac{2b^2(\alpha+\gamma)}{\left(q^2-(\alpha b)^2\right)(q+\gamma b)} - \exp(-qz) + c_2\exp(-q(1-z)) \quad (32)$$

At the bottom position with $z = 1$, the derivative of the equation according to z means:

$$\frac{\partial \bar{v}}{\partial z} = -\frac{2\alpha b^2}{q^2-(\alpha b)^2}\exp(-\alpha b) + \frac{2b^2(\alpha+\gamma)q}{\left(q^2-(\alpha b)^2\right)(q+\gamma b)}\exp(-q) + c_2 q \quad (33)$$

The rear boundary condition can be presented by Eq. (34):

$$\frac{\partial \bar{v}}{\partial z} = \bar{\nu}\gamma b;\ z = 1;\ \tau > 0 \quad (34)$$

The combination of Eqs. (33) and (34) leads to:

$$-\frac{2\alpha b^2 e^{-\alpha b}}{q^2-(\alpha b)^2} + \frac{2b^2(\alpha+\gamma)qe^{-q}}{\left(q^2-(\alpha b)^2\right)(q+\gamma b)} + c_2 q = \frac{2b^2\gamma e^{-\gamma b}}{q^2-(\alpha b)^2} - \frac{2b^3\gamma(\alpha+\gamma)e^{-q}}{\left(q^2-(\alpha b)^2\right)(q+\gamma b)} + c_2\gamma b \quad (35)$$

After rearrangement we obtain for c_2 the expression:

$$c_2 = \frac{2b^2(\alpha+\gamma)e^{-\alpha b}}{\left(q^2-(\alpha b)^2\right)(q-\gamma b)} - \frac{2b^2(\alpha+\gamma)e^{-q}}{\left(q^2-(\alpha b)^2\right)(q-\gamma b)} \quad (36)$$

With Eq. (36) the solution of Eq. (32) can be presented by:

$$\bar{v} = \frac{2be^{-z\alpha b}}{q^2-(\alpha b)^2} - \frac{2b^2(\alpha+\gamma)e^{-qz}}{\left(q^2-(\alpha b)^2\right)(q+\gamma b)} + \frac{2b^2(\alpha+\gamma)e^{-\alpha b}e^{-q(1-z)}}{\left(q^2-(\alpha b)^2\right)(q-\gamma b)} - \frac{2b^2(\alpha+\gamma)e^{-q(2-z)}}{\left(q^2-(\alpha b)^2\right)(q-\gamma b)} \quad (37)$$

The back transformation after splitting in partial fractions leads at first to the v function:

$$v = \exp\left(\frac{\alpha^2\tau - 2z\alpha}{4ae}\right) - \frac{a}{2e}\exp\left(\frac{\alpha^2\tau + 2\alpha z}{4ae}\right)\operatorname{erfc}\left(\frac{z+\alpha\tau}{2\sqrt{ae\tau}}\right) - \frac{1}{2}\exp\left(\frac{\alpha^2\tau - 2z\alpha}{4ae}\right)\operatorname{erfc}\left(\frac{z-\alpha\tau}{2\sqrt{ae\tau}}\right) + \frac{\gamma}{2e}\exp\left(\frac{\gamma^2\tau + 2z\gamma}{4ae}\right)\operatorname{erfc}\left(\frac{z+\gamma\tau}{2\sqrt{ae\tau}}\right) - \frac{1}{2}\exp\left(\frac{\alpha^2\tau + 2\alpha(1-z) - 2\alpha}{4ae}\right) \times \operatorname{erfc}\left(\frac{(1-z)+\alpha\tau}{2\sqrt{ae\tau}}\right) - \frac{a}{2e}\exp\left(\frac{\alpha^2\tau - 2\alpha(1-z) - 2\alpha}{4ae}\right) \times \operatorname{erfc}\left(\frac{(1-z)-\alpha\tau}{2\sqrt{ae\tau}}\right) + \frac{\gamma}{2e}\exp\left(\frac{\gamma^2\tau - 2\gamma(1-z) - 2\alpha}{4ae}\right) \times \operatorname{erfc}\left(\frac{(1-z)-\gamma\tau}{2\sqrt{ae\tau}}\right)$$

$$+\frac{1}{2}\exp\left(\frac{\alpha^2\tau+2\alpha(2-z)}{4ae}\right)\mathrm{erfc}\left(\frac{(2-z)+\alpha\tau}{2\sqrt{ae\tau}}\right)$$

$$+\frac{a}{2e}\exp\left(\frac{\alpha^2\tau-2\alpha(2-z)}{4ae}\right)\mathrm{erfc}\left(\frac{(2-z)-\alpha\tau}{2\sqrt{ae\tau}}\right)$$

$$-\frac{\gamma}{2e}\exp\left(\frac{\gamma^2\tau-2\gamma(2-z)}{4ae}\right)\mathrm{erfc}\left(\frac{(2-z)-\gamma\tau}{2\sqrt{ae\tau}}\right) \quad (38)$$

Now the function for the radial concentration distribution reads:

$$C=\frac{C_0}{2}e^{-\tau}\Bigg\{2-\mathrm{erfc}\left(\frac{z-\tau\alpha}{2\sqrt{ae\tau}}\right)$$

$$-\frac{a}{e}\exp\left(\frac{z\alpha}{ae}\right)\mathrm{erfc}\left(\frac{\tau\alpha+z}{2\sqrt{ae\tau}}\right)$$

$$+\frac{\gamma}{e}\exp\left(\frac{(\gamma^2-\alpha^2)\tau+2z(\alpha+\gamma)}{4ae}\right)$$

$$\times\mathrm{erfc}\left(\frac{\tau\gamma+z}{2\sqrt{ae\tau}}\right)-\mathrm{erfc}\left(\frac{1-z+\alpha\tau}{2\sqrt{ae\tau}}\right)$$

$$-\frac{a}{e}\exp\left(\frac{-\alpha(1-z)}{ae}\right)\mathrm{erfc}\left(\frac{1-z-\alpha\tau}{2\sqrt{ae\tau}}\right)$$

$$+\frac{\gamma}{e}\exp\left(\frac{(\gamma^2-\alpha^2)\tau-2(\alpha+\gamma)(1-z)}{4ae}\right)$$

$$\times\mathrm{erfc}\left(\frac{1-z-\gamma\tau}{2\sqrt{ae\tau}}\right)$$

$$+\exp\left(\frac{\alpha}{ae}\right)\mathrm{erfc}\left(\frac{2-z+\alpha\tau}{2\sqrt{ae\tau}}\right)$$

$$+\frac{a}{e}\exp\left(\frac{-\alpha(1-z)}{ae}\right)$$

$$\times\mathrm{erfc}\left(\frac{2-z-\alpha\tau}{2\sqrt{ae\tau}}\right)$$

$$-\frac{\gamma}{e}\exp\left(\frac{(\gamma^2-\alpha^2)\tau+2z(\alpha+\gamma)-4y}{4ae}\right)$$

$$\times\mathrm{erfc}\left(\frac{2-z-\gamma\tau}{2\sqrt{ae\tau}}\right)\Bigg\} \quad (39)$$

In a more simplified manner, the concentration distribution function can be expressed as follows:

$$C=\frac{C_0}{2}e^{-\tau}\Bigg\{2-\mathrm{erfc}\left(\frac{z-\tau\alpha}{2\sqrt{ae\tau}}\right)$$

$$-\frac{a}{e}\exp\left(\frac{z\alpha}{ae}\right)\mathrm{erfc}\left(\frac{\tau\alpha+z}{2\sqrt{ae\tau}}\right)$$

$$+\frac{\gamma}{e}\exp\left(\frac{e\tau+z}{e}\right)\mathrm{erfc}\left(\frac{\tau\gamma+z}{2\sqrt{ae\tau}}\right)$$

$$-\mathrm{erfc}\left(\frac{1-z+\alpha\tau}{2\sqrt{ae\tau}}\right)$$

$$-\frac{a}{e}\exp\left(\frac{-\alpha(1-z)}{ae}\right)\mathrm{erfc}\left(\frac{1-z-\alpha\tau}{2\sqrt{ae\tau}}\right)$$

$$+\frac{\gamma}{e}\exp\left(\frac{e\tau-1+z}{e}\right)\mathrm{erfc}\left(\frac{1-z-\gamma\tau}{2\sqrt{ae\tau}}\right)$$

$$+\exp\left(\frac{\alpha}{ae}\right)\mathrm{erfc}\left(\frac{2-z+\alpha\tau}{2\sqrt{ae\tau}}\right)$$

$$+\frac{a}{e}\exp\left(\frac{-\alpha(1-z)}{ae}\right)\mathrm{erfc}\left(\frac{2-z-\alpha\tau}{2\sqrt{ae\tau}}\right)$$

$$-\frac{\gamma}{e}\exp\left(\frac{e\tau+z-\gamma/a}{e}\right)\mathrm{erfc}\left(\frac{2-z-\gamma\tau}{2\sqrt{ae\tau}}\right)\Bigg\} \quad (40)$$

Eq. (40) contains nine complementary error functions. However, the numerical examination demonstrates a noticeable influence of the last three complimentary error functions on the accuracy of the solution only in cases with very long experimental time and very high diffusion coefficients. Therefore, these error functions can be neglected.

When using $z=0.5$ in Eq. (9), as the mean value of the integration region, the solution with the remaining six error functions is identical with the Fujita equation (Eq. 2.280 in Ref. [8] or here Eq. (41)) as one can recognize after introduction of the same mathematical symbols. In the publication of

Fujita [8], there is no information about the derivation of this solution.

$$C = \frac{C_0}{2} e^{-\tau} \left\{ 2 - \operatorname{erfc}\left(\frac{z - \tau\alpha}{2\sqrt{ae\tau}} \right) - \frac{a}{e} \exp\left(\frac{z\alpha}{ae} \right) \operatorname{erfc}\left(\frac{\tau\alpha + z}{2\sqrt{ae\tau}} \right) + \frac{\gamma}{e} \exp\left(\frac{e\tau + z}{e} \right) \operatorname{erfc}\left(\frac{\tau\gamma + z}{2\sqrt{ae\tau}} \right) - \operatorname{erfc}\left(\frac{1 - z + \alpha\tau}{2\sqrt{ae\tau}} \right) - \frac{a}{e} \exp\left(\frac{-\alpha(1 - z)}{ae} \right) \operatorname{erfc}\left(\frac{1 - z - \alpha\tau}{2\sqrt{ae\tau}} \right) + \frac{\gamma}{e} \exp\left(\frac{e\tau - 1 + z}{e} \right) \operatorname{erfc}\left(\frac{1 - z - \gamma\tau}{2\sqrt{ae\tau}} \right) \right\} \quad (41)$$

With the symbols:

$$x = \left(\frac{r}{r_0} \right)^2 \qquad x_b = \left(\frac{r_b}{r_0} \right)^2 \qquad z = \frac{x - 1}{x_b - 1}$$

$$e = \frac{\varepsilon}{x_b - 1} \qquad a = \frac{1 + x_b}{2(x_b - 1)} \qquad \alpha = a - e$$

$$\gamma = a + e$$

The comparison of the six-membered solution Eq. (41) for both boundary conditions with the two solutions for only one boundary condition (Eqs. (25) and (31)) indicates that the final solution Eq. (41) is the sum of the two particular solutions. The initial concentration C_0 symbolized by the first term (value 2) in both equations, however, must be deleted once (see Fig. 1). This means that the first three terms of the six-membered solution fulfill the initial and meniscus boundary conditions, whereas the last three terms fulfill the bottom boundary condition. This circumstance offers the possibility to introduce different values for the parameter a for both halves of Eq. (41). The parameter a (Eq. (9)) depends on the constant value chosen for the explicit integration variable z. In the Fujita solution, this value amounts to 0.5. A more precise solution of the Lamm equation may be obtained if the value of the variable z in the first half of Eq. (41) depends on the midpoint position (r_*) of the moving boundary as already considered for the improved Fujita–MacCosham solution [9]. For the second half of Eq. (41), which describes the steep concentration rise near the bottom, the value of z may be chosen to 1. Both boundary conditions are fulfilled for any chosen value of z or a.

For the first three terms of Eq. (41), we define the parameter a_1:

$$a_1 = \frac{1 + (\exp(\tau) - 1) * 0.5}{x_b - 1}$$

$$z = \frac{(e^{\tau - 1}) * 0.5}{x_b - 1} \quad (42)$$

For travelling the midpoint position of the moving boundary we adopt the relation $(r_*/r)^2 = \exp(\tau)$ [12].

For the last three terms of Eq. (41) the parameter a_2 ($z = 1$) reads:

$$a_2 = \frac{x_b}{x_{b-1}} \quad (43)$$

Eq. (41) is then transformed to:

$$c = \frac{c_0}{2} e^{-\tau} \left\{ 2 - \operatorname{erfc}\left(\frac{z - \tau\alpha_1}{2\sqrt{a_1 e\tau}} \right) - \frac{a_1}{e} \exp\left(\frac{z\alpha_1}{a_1 e} \right) \operatorname{erfc}\left(\frac{\tau\alpha_1 + z}{2\sqrt{a_1 e\tau}} \right) + \frac{\gamma_1}{e} \exp\left(\frac{e\tau + z}{e} \right) \operatorname{erfc}\left(\frac{\tau\gamma_1 + z}{2\sqrt{a_1 e\tau}} \right) - \operatorname{erfc}\left(\frac{1 - z + \alpha_2\tau}{2\sqrt{a_2 e\tau}} \right) - \frac{a_2}{e} \exp\left(\frac{-\alpha_2(1 - z)}{a_2 e} \right) \operatorname{erfc}\left(\frac{1 - z - \alpha_2\tau}{2\sqrt{a_2 e\tau}} \right) + \frac{\gamma_2}{e} \exp\left(\frac{e\tau - 1 + z}{e} \right) \operatorname{erfc}\left(\frac{1 - z - \gamma_2\tau}{2\sqrt{a_2 e\tau}} \right) \right\} \quad (44)$$

with the additional symbols:

$$\alpha_1 = a_1 - e \qquad \gamma_1 = a_1 + e$$

$$\alpha_2 = a_2 - e \qquad \gamma_2 = a_2 + e$$

The different definition of the parameters a_1 and a_2, respectively, the two values of z for the two halves of Eq. (41) raises the accuracy of the solution considerably.

3. Material and methods

The oligo-peptides angiotensin I and II were obtained from Sigma Chemical. Sedimentation velocity runs were carried out with an XL-A ultracentrifuge (Beckman Instruments, Palo Alto, CA) equipped with UV absorbance optics. For all experiments, conventional double sector cells were used. In addition to the experimental curves, noise-free data derived from the finite element method [13] were analyzed for the simultaneous determination of sedimentation and diffusion coefficients. Radial concentration profiles were calculated for proteins of various molecular masses, starting with the parameters of $s = 40$ S and $D = 1 \times 10^{-7}$ cm^2/s until low molecular mass compounds with $s = 0.2$ S and $D = 3 \times 10^{-6}$ cm^2/s. Different speeds among 10,000 and 60,000 rpm were used adequately for the expected sedimentation velocity of the macromolecules. The curves between the meniscus radius $r_0 = 6.4$ cm and the cell base $r_b = 7.2$ cm were represented by 1600 data points with a radial step length of 0.0005 cm and a simulation time step of $dt = 0.5$ s.

The sedimentation and diffusion coefficients were estimated simultaneously by a nonlinear fitting procedure using Eq. (41), which is identical to the old variant derived by Fujita [8], and the improved function (Eq. (44)). A computer program, Lamm, was written in Turbo Pascal 7.0 running under MS-DOS on a Pentium personal computer. The program reads up to 18 XL-A data files and fits them simultaneously (global fit). All further details of the program and the numerical methods used for the calculation of the estimated parameters are published [9].

Sedimentation and diffusion coefficients together with the partial specific volume $\bar{\nu}$ allow us to calculate the molecular mass M.

$$M = \frac{s \cdot R \cdot T}{D(1 - \rho\bar{v})} \tag{45}$$

Here, R is the gas constant, T the absolute temperature and ρ the solvent density. Using the molecular mass, the partial specific volume and the Avogadro number N_A we obtain the volume V of the dry macromolecule.

$$V = M\bar{\nu}/N_A \tag{46}$$

Furthermore, sedimentation and diffusion coefficient allow us to determine also the complex parameter describing the frictional ratio $(f/f_0)_t$

$$\left(\frac{f}{f_0}\right)_t = 10^{-8}\left(\frac{1 - \rho\bar{\nu}}{sD^2\bar{v}}\right)^{1/3} \tag{47}$$

that contains a shape and a hydration dependent part $(f/f_0)_h$. The latter can be calculated from the average amount of water (w) molecules which are in contact with the substance of interest.

$$\left(\frac{f}{f_0}\right)_h = \left(1 + \frac{w}{\rho\bar{v}}\right)^{1/3} \tag{48}$$

For proteins of different size an average value of about 0.3 g water/g solute was communicated by Pessen and Kumosinski [14]. Taking into account this data from the remaining shape-dependent part of the frictional ratio, we can estimate the half axes of an ellipsoid of revolution or the maximal length (L) and the diameter (d) of the macromolecule.

Independently from this procedure, we have modeled the peptide structure of Ang I and Ang II by the program Quanta, version 3.3 (Molecular Simulations, Waltham MA) to compare the dimensions derived from the ultracentrifugation experiments.

CD measurements of the angiotensin peptides were recorded on a Jasco J-720 spectropolarimeter calibrated with D-10-camphorsulfonic acid. Mean residue ellipticities $[\Theta]$ were calculated using a mean residue mass of 110 Da. CD spectra were measured with a 0.1 cm cell.

4. Results

4.1. Fitting of noise-free synthetic data

Because the approximate solution of the Lamm equation (Eq. (41)) is of the Archibald type and therefore particularly well suited to estimate the sedi-

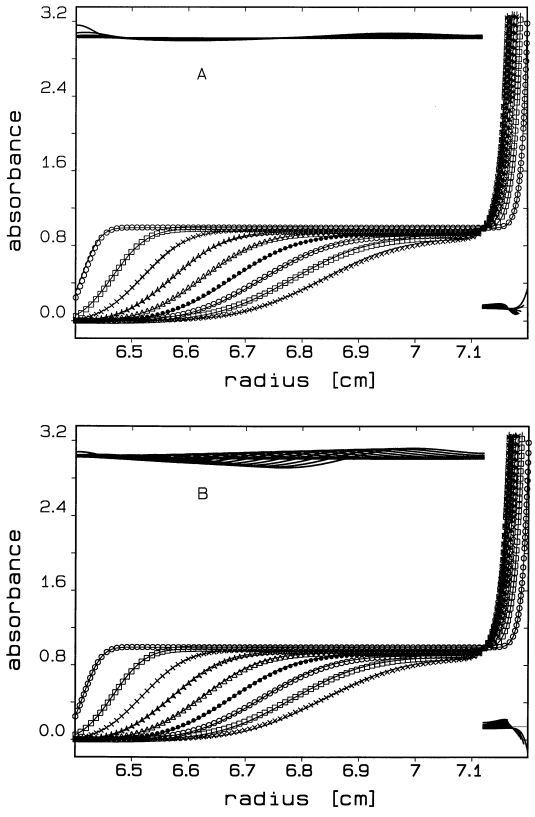

Fig. 2. Claverie simulation obtained for $s = 2$ S and $D = 8 \times 10^{-7}$ cm^2/s at 50 000 rpm (conventional double sector cell). (A) Fit using Eq. (41) and (B) by Eq. (44). Residuals are given in twofold (A) or eightfold (B) amplification. Estimated values: (A) $C_0 = 0.9965$, $s = 1.903$ S, $D = 7.773 \times 10^{-7}$ cm^2/s, $r_0 = 6.3946$ cm, $r_b = 7.1982$ cm; (B) $C_0 = 0.9978$, $s = 2.006$ S, $D = 8.061 \times 10^{-7}$ cm^2/s, $r_0 = 6.3995$ cm, $r_b = 7.2001$ cm.

mentation and diffusion coefficients of low molecular mass compounds, we first analyzed concentration distribution curves obtained for $s = 2$ S and $D = 8 \times 10^{-7}$ cm^2/s. For the fitting procedure, Eq. (41) and the improved function Eq. (44) have been used. Eq. (41) yields a reasonable fit (Fig. 2A). Although this function accounts to the boundary at the meniscus position, the fit in this region is not optimal, resulting in sedimentation and diffusion coefficients that are too low by about 6 or 4%, respectively. However, with respect to the molecular mass, the deviation of the expected value amounts to only about 2%. In contrast to this, the improved function Eq. (44) fits the curves more accurately (Fig. 2B). Both parameters (s and D) are estimated nearly optimally and deviate less than 1% from the expected data. Inevitably for the molecular mass, an accurate value is obtained.

To compare the efficiency of both model functions for extremely low molecular mass substances, the radial concentration distribution curves for $s = 0.2$ S and $D = 3 \times 10^{-6}$ cm^2/s were analyzed (Fig. 3A,B). Whereas the sedimentation coefficient was found about 2% too low using the original Fujita version (Eq. (41)), for the improved variant (Eq. (44)), we obtained a sedimentation coefficient about 1% too high. With respect to the diffusion coefficients, the deviations are considerably smaller or result in the expected values. Therefore, the calcu-

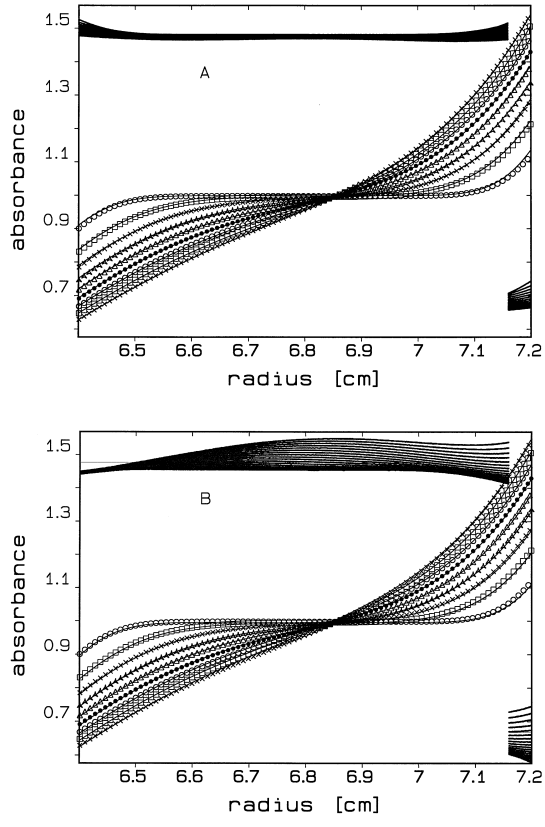

Fig. 3. Fits of the Claverie simulation obtained for $s = 0.2$ S and $D = 3 \times 10^{-6}$ cm^2/s at 60 000 rpm using Eq. (41) for (A) and Eq. (44) for (B). In both cases, the residuals are given in eightfold amplification. Estimated values: (A) $C_0 = 1.0009$, $s = 0.1966$ S, $D = 3.014 \times 10^{-6}$ cm^2/s, $r_0 = 6.3906$ cm, $r_b = 7.1884$ cm; (B) $C_0 = 0.9975$, $s = 0.2008$ S, $D = 2.980 \times 10^{-6}$ cm^2/s, $r_0 = 6.4022$ cm, $r_b = 7.2050$ cm.

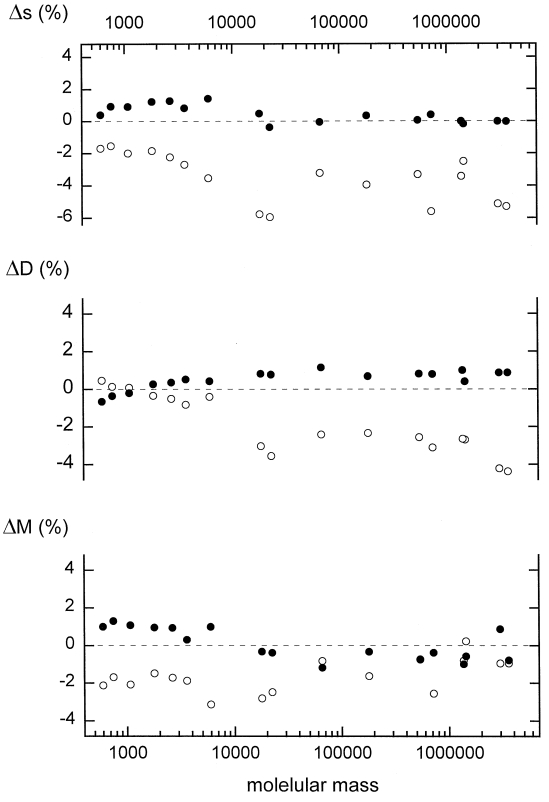

Fig. 4. Plots of the deviations of estimated sedimentation and diffusion coefficients and molecular masses in dependence of the size of macromolecules. The calculation of the parameters from the synthetic curves (Claverie simulations) were obtained: (∘) using Eq. (41) or (•) by Eq. (44).

lated molecular mass reflects the same deviations as observed for the sedimentation coefficients.

The curve analysis for substances with a molecular mass up of to 3.5 millions Da results in sedimentation and diffusion coefficients that are too small by 4–5% using Eq. (41). The deviations in the calculated molecular masses, however, are considerably lower (see Fig. 4). The improved function, Eq. (44) yields the expected sedimentation coefficients, but the diffusion coefficients are too high on average by about 1%. Therefore, most of the corresponding molecular mass data is too small by the same amount.

4.2. Analysis of experimental curves

Because the model functions discussed here are particularly suitable for the simultaneous estimation of sedimentation and diffusion coefficients of low molecular mass substances, we have studied the sedimentation behavior of peptides such as Ang I or Ang II, consisting of 10 or 8 amino acids, respectively. Fig. 5 shows the concentration distribution curves of the peptide Ang II which are fitted well by Eq. (44). From the estimated parameters of $s_{20,w} = 0.291$ S, $D_{20,w} = 2.42 \times 10^{-6}$ cm^2/s considering a partial specific volume $\bar{v} = 0.731_7$ ml/g, a molecular mass $M = 1087$ was calculated using Eq. (45). This indicates that the dissolved peptide exists in the monomeric state. Similar results were obtained when fitting the curves using Eq. (41). Table 1 shows the average values of at least 6 single experiments for angiotensin I and II analyzed by both Eqs. (41) and (44). Generally we can establish, in comparison with Eq. (41), that the application of the improved Eq. (44) leads to slightly higher sedimentation coefficients. The estimated diffusion coefficients were found to be nearly equally independent from the fitting function. The molecular mass data obtained from Eq. (44) are closer to the expected values as those derived from Eq. (41).

By means of the sedimentation and diffusion coefficients in combination with the partial specific volume, we can calculate the frictional ratio f/f_0 of macromolecules using Eq. (47) and the shape-dependent part considering Eq. (48). This value allows us to draw some conclusion about the gross conforma-

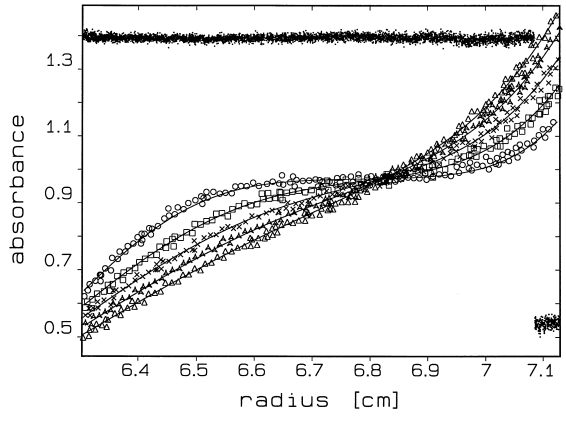

Fig. 5. Radial concentration distributions obtained for 0.6 mg/ml Ang II dissolved in 50 mM K–phosphate buffer, pH 7.0, containing 150 mM NaCl. From the 15 records used for the calculation, only each third is presented. Residuals are given in twofold amplification.

Table 1
Hydrodynamic parameters of Ang I and Ang II derived by Eqs. (41) and (44) in 50 mM K–phosphate buffer, pH 7.0, containing 150 mM NaCl

Substance	Equation	$s_{20,w}$ (S)	$D_{20,w}$ (10^7 cm^2/s)	M (Da)	f/f_0	ΔM (%)
Ang I	Eq. (41)	0.288 ± 0.006	22.29 ± 0.53	1204 ± 54	1.35 ± 0.03	-7.1
Ang I	Eq. (44)	0.320 ± 0.004	22.54 ± 0.33	1323 ± 36	1.29 ± 0.02	$+2.1$
Ang II	Eq. (41)	0.275 ± 0.005	24.77 ± 0.56	1004 ± 41	1.30 ± 0.03	-4.0
Ang II	Eq. (44)	0.296 ± 0.007	24.69 ± 0.37	1084 ± 42	1.27 ± 0.02	$+3.6$

ΔM is the deviation from the theoretical molecular mass: 1296 Da for Ang I, and 1046 for Ang II.

tion of the substances analyzed here. The f/f_0 data calculated for the angiotensin peptides are slightly smaller when using the s and D values obtained by Eq. (44). From these data, it seems that the peptides are slightly more sphere-like as when using the results from the original model function (Eq. (41)). In comparison with the octa-peptide Ang II the deca-peptide Ang I possess a somewhat higher f/f_0 value. From this result, we can conclude the peptide chain of Ang I is prolonged by two further amino acids without backfolding. Assuming a prolate ellipsoid of revolution for both peptides and an averaged hydration of 0.3 g $H_20/$ g peptide, we can calculate axial ratios $L{:}d$ of 4.0 for Ang I and 3.4 for Ang II. Using Eq. (46), a dry volume of 1.59 nm^3 for Ang I and 1.27 nm^3 for Ang II were calculated. In combination with the axial ratios, the following average dimensions for the peptide length (L) and the diameter (d) can be obtained: $L = 3.65$ nm, $d = 0.91$ nm (Ang I) and $L = 3.04$ nm, $d = 0.89$ nm (Ang II). The data for L agree very well with those of 3.7 nm (Ang I) or 3.05 nm (Ang II) obtained by computer simulation with a discrete water content and using the program Quanta.

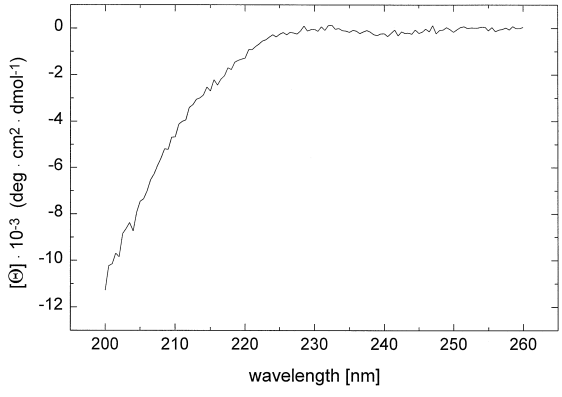

Fig. 6. CD spectrum of Ang I (0.2 mg/ml) dissolved in 50 mM K–phosphate buffer, pH 7.0, containing 150 mM NaCl.

To fill the volume with the proposed dimensions, the peptides are expected to adopt an extended chain conformation without a possible backfolding or defined secondary structure in solution. To check whether the above proposed unordered structure for the Ang peptides in the aqueous solution is realistic, we have carried out additionally CD measurements. Both CD spectra of Ang I (see Fig. 6), as well as of Ang II (not shown) are characterized by a steady rise of ellipticities with increasing wavelength typically for proteins and peptides with missing higher-order structure.

5. Discussion

Sedimentation and diffusion coefficients are important parameters to characterize size and shape of macromolecules in solution. There is a particular interest of the biotechnology to provide information about the molecular mass and homogeneity or especially to the conformation of low molecular mass compounds such as cytokines, growth factors, etc. Moreover, it is desirable to know the details about peptide ligands as structural motives that are involved in the protein–protein interaction. Because of the broad boundaries produced by the low molecular mass compounds with high diffusion coefficients, it is difficult to recognize additional species in sedimentation experiments. To overcome this difficulty, approximate solutions of the Lamm equation are useful. They allow us to estimate simultaneously sedimentation and diffusion coefficients from sedimentation velocity experiments. It is to the credit of

Fujita [8], that more than 30 years ago, he derived some model functions to fit the radial concentration distribution curves. The development of powerful computers in the last years was a prerequisite for the extensive application of these equations. After having some effort to develop another approximate solution of the Lamm equation by Holladay [10] recently, Philo [15,17] and we [9] have used the model functions derived by Fujita [8,12] for routine analysis, and have published our experience with these model functions. To obtain more accurate results particularly for low molecular mass proteins, the Fujita–MacCosham equation [16] was improved by two additional empirically determined factors [17] or by introducing a time-dependent factor [9].

Here, we present the derivation of an approximate solution of the Lamm equation of the Archibald type that does not require the plateau region. This equation that is partly identical with the model function given by Fujita [8] allows one to analyze also extremely low molecular mass substances of about 1 kDa. However, the explicit integration variable z requires various values for the two parts of the six-membered equation describing the different parts of the curves. When considering this, we obtained an improved function that yields a more optimal fit than the old variant of Fujita [8] and Behlke and Ristau [9] for which z is held constantly at 0.5. The more accurate parameters allow us to analyze macromolecules covering a broad range of molecular masses from some million Daltons to small peptides of about eight amino acids for which the approximate solutions of the Faxén type fail.

The knowledge of sedimentation and diffusion coefficients gives us the opportunity to estimate the gross conformation. Assuming that angiotensin is normally hydrated (0.3 water/g solute), we can estimate the peptide length from the frictional ratio, which indicate that Ang I and Ang II form extended chains in solution. The CD spectra of the peptides confirm this result. It is of particular interest to have some information about the molecular dimensions of biological active peptides as Ang I, and especially Ang II which exerts physiological actions on cardiovascular regulation and fluid homeostasis by binding to type 1 Ang receptors (AT1 receptors) in the plasma membrane of smooth muscle adrenal renal and neural cells [18]. Ang II receptor type 1 shows characteristic features of a G protein coupled, seven-transmembrane receptor with three cytosolic and three extracellular loops. Much less is known about the structure function properties of receptors that bind Ang II [19]. Mutational studies on the AT1 receptor published recently describe the amino acids that are in contact with Ang II. Noda et al. [20] have demonstrated that Lys 199 in the transmembrane helix V of the AT1 receptor binds the COOH-terminal alpha carboxyl group of Ang II. Feng et al. [21] have shown that the amino acids His 183 located in the extracellular domain between the helices IV and V or Asp 281 from helix VII of the AT1 receptor are involved in binding the NH_2-terminal Asp1 and Arg2 residues of Ang II. Furthermore, the conserved Asn 111 from the helix III was shown is able to interact with Tyr4 of Ang II [22]. Computer simulations [23] to get insight in the optimal packing shape of the δ opioid receptor that is related to the AT1 receptor indicate a 7-helix bundle structure with an oval arrangement of the helices. Assuming a similar structure of the AT1 receptor allows a contact of Ang II with the above-mentioned critical amino acids only for an extended chain conformation of the Ang II peptide.

Based on our experimental data in solution, both peptides should exist as extended chains. Their lengths of 3.65 nm for Ang I and 3.04 nm for Ang II agree well with data derived by computer simulation using the program Quanta that allows one to consider water molecules in the surroundings of the peptides (data not shown). Under the assumption that no drastic conformational changes take place during the binding of Ang II, the AT1 receptor should form a narrow binding cleft in a position nearly parallel to the plasma membrane similar as described recently for the related opioid receptor [23].

The improved approximate solution of the Lamm equation will be used for the analysis of other biological active peptides, in particular those that are involved in protein–protein interactions of certain complexes.

Acknowledgements

The authors are grateful to Mrs. Bärbel Bödner for the skillful technical assistance, and to Mr. W.

Leistner for the support in modeling the peptide structures.

References

[1] S.E. Harding, A.J. Rowe, J.C. Horton (Eds.), Analytical Ultracentrifugation in Biochemistry and Polymer Science, R. Soc. Cambridge, UK, 1992.
[2] T.M. Schuster, T.M. Laue (Eds.), Modern Analytical Ultracentrifugation, Birkhäuser, Boston, 1994.
[3] D. Brune, S. Kim, Proc. Natl. Acad. Sci. U.S.A. 90 (1993) 3835.
[4] J.A. McCammon, S.C. Harvey, Dynamics of Proteins and Nucleic Acids, Cambridge Univ. Press, Cambridge, UK, 1987.
[5] S.H. Northrup, Curr. Opin. Struct. Biol. 4 (1994) 269.
[6] R.R. Gabdoulline, R.C. Wade, Biophys. J. 72 (1997) 1917.
[7] O. Lamm, Ark. Mat. Astr. Fys. 21B (1929) 1.
[8] H. Fujita, Mathematical Theory of Sedimentation Analysis, Academic Press, New York, 1962.
[9] J. Behlke, O. Ristau, Biophys. J. 72 (1997) 428.
[10] L.A. Holladay, Biophys. Chem. 10 (1979) 187.
[11] H.S. Carslow, J.C. Jaeger, Conduction of Heat in Solids, Oxford Univ. Press, London, 1986.
[12] H. Fujita, Foundations of Ultracentrifugal Analysis, Wiley, New York, 1975.
[13] J.M. Claverie, H. Dreux, R. Cohen, Biopolymers 14 (1975) 1685.
[14] H. Pessen, T.F. Kumosinski, Methods Enzymol. 117 (1985) 219.
[15] J.S. Philo, in: T.M. Schuster, T.M. Laue (Eds.), Modern Analytical Ultracentrifugation, Birkhäuser, Boston, 1994, p. 156.
[16] H. Fujita, V.J. MacCosham, J. Chem. Phys. 30 (1959) 291.
[17] J.S. Philo, Biophys. J. 72 (1997) 435.
[18] K.J. Catt, K. Sandberg, T. Balka, Cellular and Molecular Biology of the Renin–Angiotensin System, CRC Press, Boca Raton, FL, 1993, p. 307.
[19] K. Sasaki, Y. Yamono, S. Bardhan, N. Iwai, J.J. Murray, M. Hasegawa, Y. Matsuda, T. Inagami, Nature 351 (1991) 230.
[20] K. Noda, Y. Saad, A. Kinoshita, T.P. Boyle, R.M. Graham, A. Husain, S.S. Karnik, J. Biol. Chem. 270 (1995) 2284.
[21] Y.H. Feng, K. Noda, Y. Saad, X.P. Liu, A. Husain, S.S. Karnik, J. Biol. Chem. 270 (1995) 12846.
[22] K. Noda, Y.H. Feng, X.P. Liu, Y. Saad, A. Husain, S.S. Karnik, Biochemistry 35 (1996) 16435.
[23] I. Alkorta, G.H. Loew, Protein Eng. 9 (1996) 573.